eLIFE
elifesciences.org

RESEARCH ARTICLE

Figures and figure supplements

CRELD1 is an evolutionarily-conserved maturational enhancer of ionotropic acetylcholine receptors

Manuela D'Alessandro *et al*

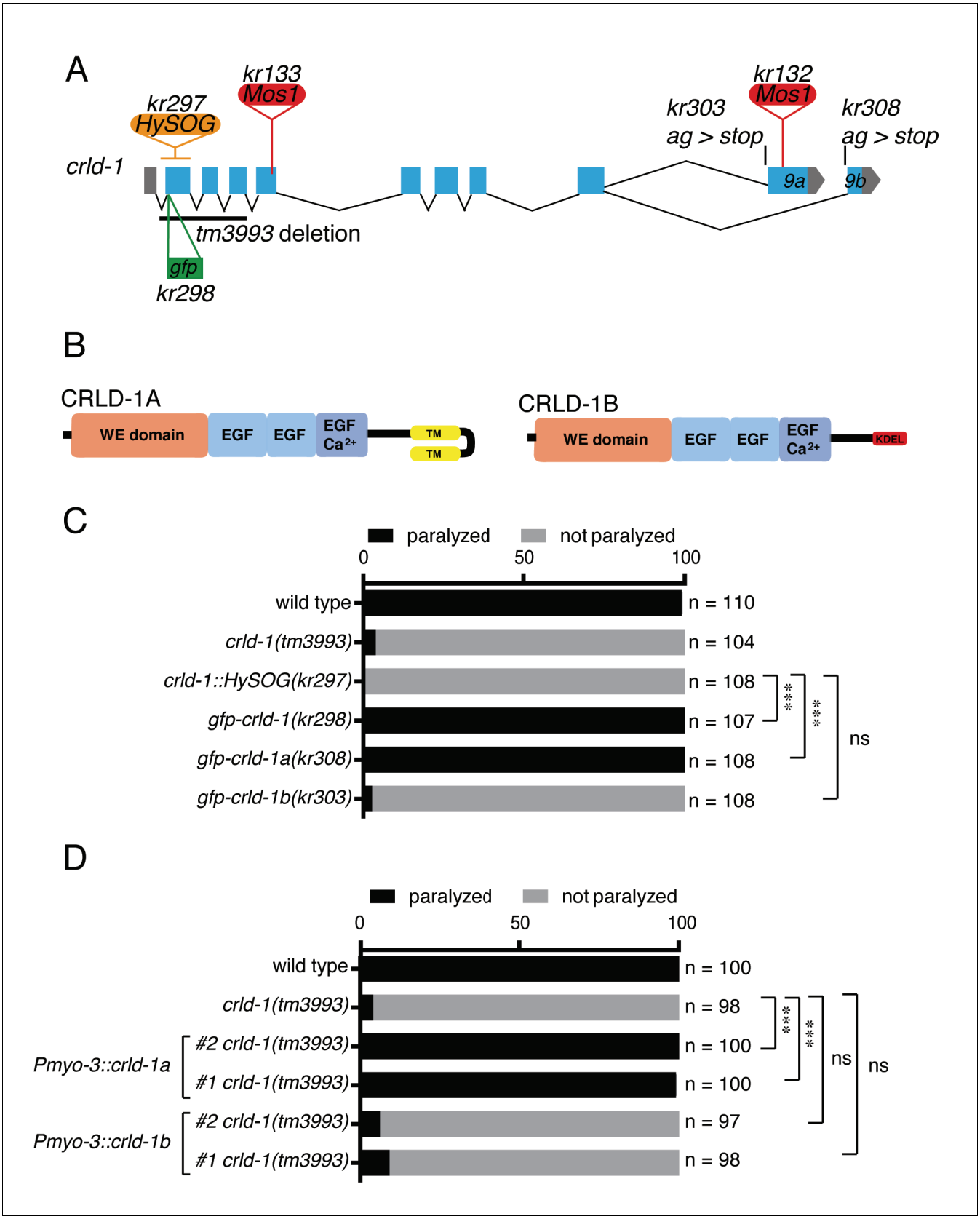

Figure 1. CRLD-1A isoform is sufficient for L-AChR expression based on sensitivity to levamisole. (**A**) Structure of the *crld-1* locus, which generates two isoforms (*crld-1a* and *crld-1b*) by alternative splicing of the last exon (exon *9a* and exon *9b*). The different *Mos1* transposon insertions and the mutant

Figure 1 continued on next page

Figure 1 continued

alleles are indicated. *kr303* and *kr308* mutations specifically express only *crld-1b* and *crld-1a*, respectively. HySOG = hygromycinB miniSOG dual selection cassette (length = 2.8 kb). The green box indicates the position of the GFP sequence inserted in the first exon of *crld-1* to generate the *gfp-crld-1(kr298)* knock-in allele. (**B**) Domain organization of CRLD-1A and CRLD-1B. SP = signal peptide, WE domain = tryptophan (**W**) and glutamic acid (**E**) enriched domain, EGF = Epidermal Growth Factor-like domain, EGF Ca^{2+} = Ca^{2+}binding epidermal growth factor-like domain, TM = transmembrane domain, KDEL = Lys-Asp-Glu-Leu ER retention signal. (**C**) *crld-1* is necessary for wild-type sensitivity to levamisole. Gray bars indicate the percentage of moving animals after overnight exposure to 1 mM levamisole, and black bars indicate the percentage of paralyzed animals. Experiments were repeated three times, n = number of animals tested. p=0,2465, ns = not significant, ***p<0.001, after Bonferroni correction, Fisher exact probability test. (**D**) Body wall muscle expression of *crld-1a* but not *crld-1b* rescues levamisole sensitivity in *creld-1(tm3993)* mutants. Gray bars indicate the percentage of moving animals after overnight exposure to 1 mM levamisole, and black bars indicate the percentage of paralyzed animals. Two independent transgenic lines were tested for each condition. Experiments were repeated four times, n = number of animals tested. p=0,2504 and 0,5369, ns = not significant, ***p<0.001, after Bonferroni correction, Fisher exact probability test.

DOI: https://doi.org/10.7554/eLife.39649.002

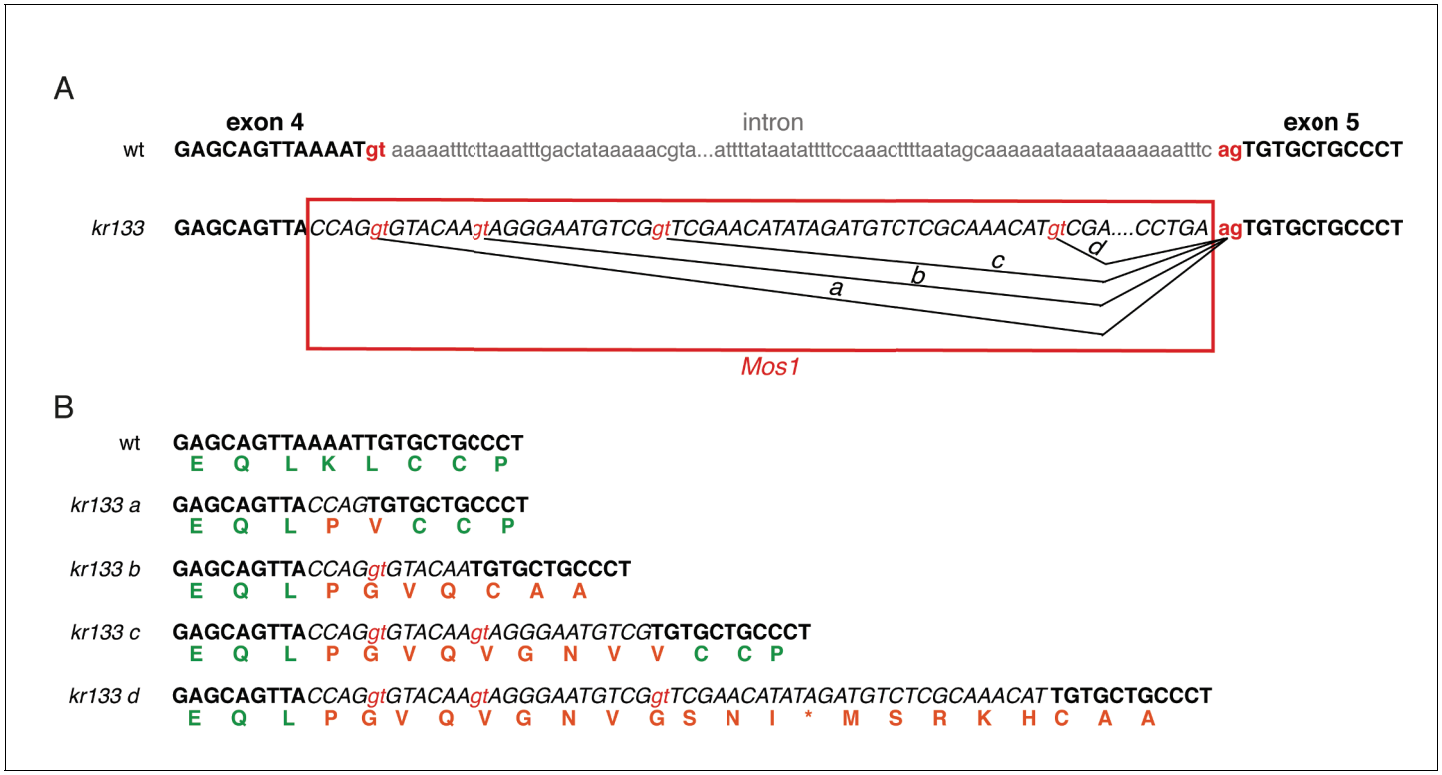

Figure 1—figure supplement 1. - Characterization of the *kr133* mutant allele. (**A**) Wild-type *crld-1* and *crld-1(kr133)* genomic loci. Only a part of the exon 4 and exon 5 sequence is shown (bold). Regions of the intron sequence (in grey) and of the *Mos1* sequence (red box) have been omitted (annotated as '. . .'). The *Mos1* insertion in *kr133* is located in the fourth exon of *crld-1*. Cryptic splice donor sites (in red) present within the *Mos1* sequence are used at low frequency to generate in-frame messenger RNAs (a, b, c and d indicated by black lines). (**B**) Alternative *crld-1* mRNAs detected by RT-PCR in *crld-1(kr133)* alleles (a, b, c, and d) and conceptual protein translations. The single-letter amino acid code is under the second nucleotide of the corresponding codon. Wild-type protein sequence is in green and mutated residues introduced by alternative splicing of the *Mos1* transposon are in orange.

DOI: https://doi.org/10.7554/eLife.39649.003

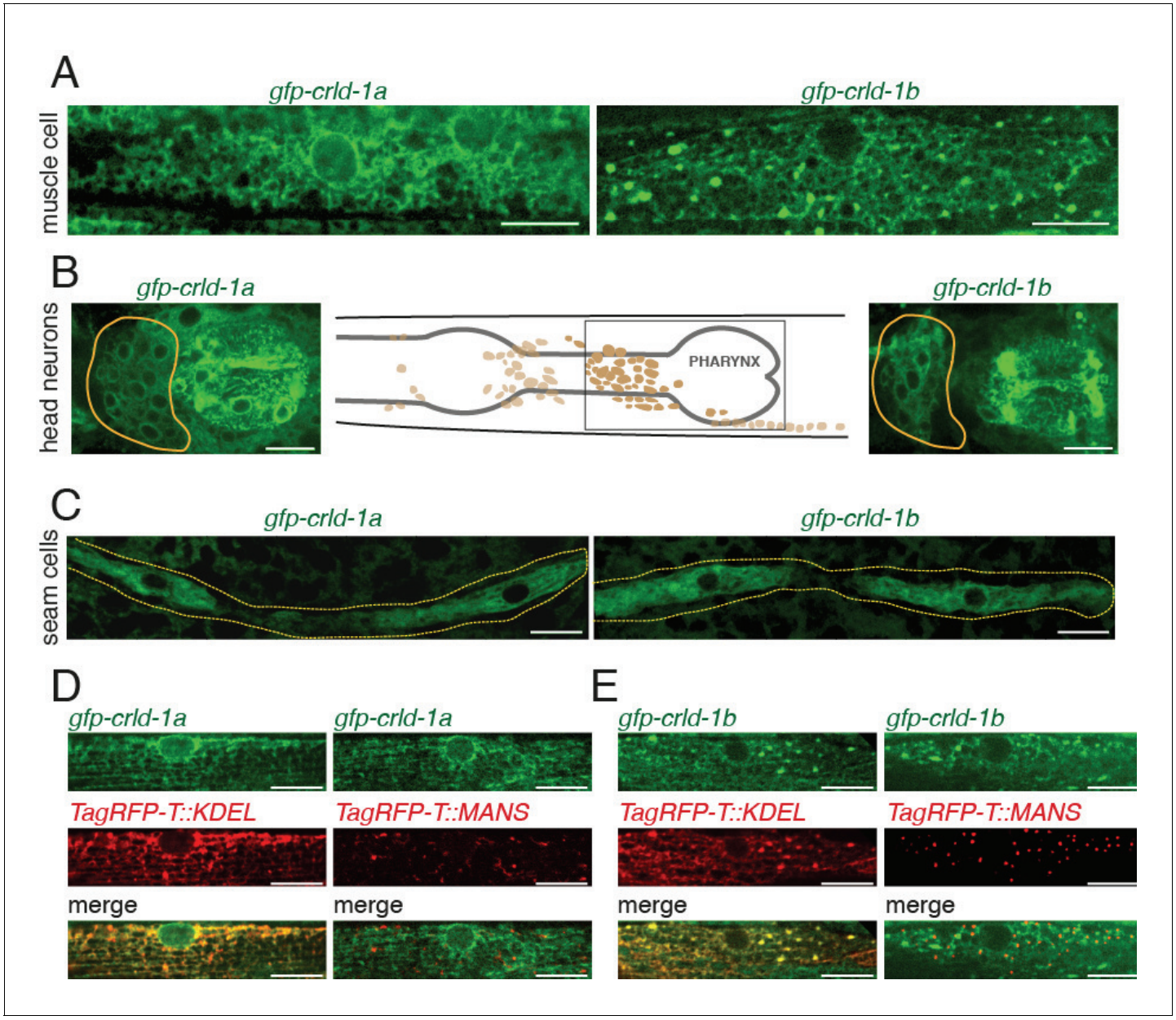

Figure 2. CRLD-1 is ubiquitously expressed and localizes in the ER of BWMs. (**A**) Distribution of GFP-CRLD-1A (left) and GFP-CRLD-1B (right) in muscle cells of *gfp-crld-1* isoform-specific knock-in worms. (**B**) Localization of CRLD-1A (left) and CRLD-1B (right) in the pharynx and in the lateral ganglion (encircled in yellow). The middle panel shows a schematic representation of the locations of neurons and ganglia in the head, adapted from: http://www.wormatlas.org/ver1/MoW_built0.92/nervous_system.html. (**C**) Localization of CRLD-1A (left) and CRLD-1B (right) in the epithelial seam cells of *gfp-crld-1* isoform-specific knock-in worms. Dashed lines, seam cell outlines. (**D**) Expression of the ER marker TagRFP-T::KDEL in *gfp-crld-1a* (left) and *gfp-crld-1b* (right) isoform-specific knock-in strains. TagRFP-T::KDEL displays a reticular pattern throughout the cytoplasm surrounding the nucleus that co-localizes with both CRLD-1A and CRLD-1B signals. (**E**) CRLD-1A and CRLD-1B from *gfp-crld-1a* (left) and *gfp-crld-1b* (right) knock-in animals do not co-localize with a Golgi-resident TagRFP-T-tagged Mannosidase II protein (MANS::TagRFP-T). In (**D**) and (**E**), the *Pmyo-3* promoter was used for expression of both TagRFP-T::KDEL and MANS::TagRFP-T in body wall muscles. In all panels, scale bars equal 10 μm.

DOI: https://doi.org/10.7554/eLife.39649.004

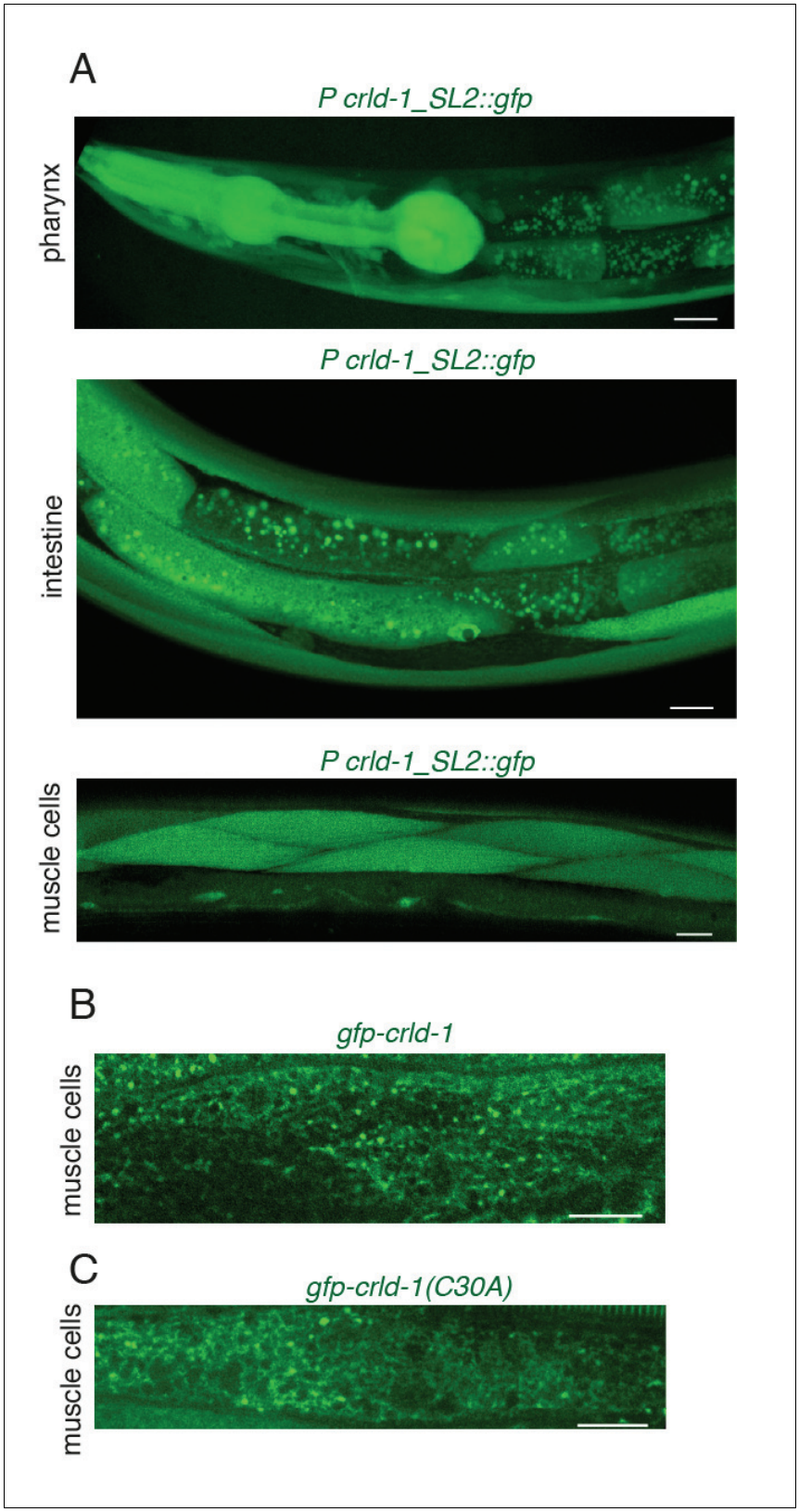

Figure 2—figure supplement 1. - CRLD-1 expression pattern. (**A**) Confocal images of transgenic animals expressing GFP under the control of *crld-1* promoter (pTB208 *Pcrld-1::SL2::gfp*). CRLD-1 is expressed in several tissues: pharynx, intestine and muscles. Scale bars: 10 µm. (**B**) Localization of CRLD-1 in muscle cells from *gfp-crld-*

Figure 2—figure supplement 1 continued on next page

Figure 2—figure supplement 1 continued

1(kr298) knock-in worms expressing both *crld-1a* and *crld-1b* isoforms. CRLD-1 reticular network is present in combination with a punctate pattern. Scale bar 10 μm. (**C**) Localization of CRLD-1 in muscle cells from *gfp-crld-1 (C30A)* knock-in worms expressing both *crld-1a* and *crld-1b* isoforms. CRLD-1 reticular network is present in combination with a punctate pattern. Scale bar: 10 μm.

DOI: https://doi.org/10.7554/eLife.39649.005

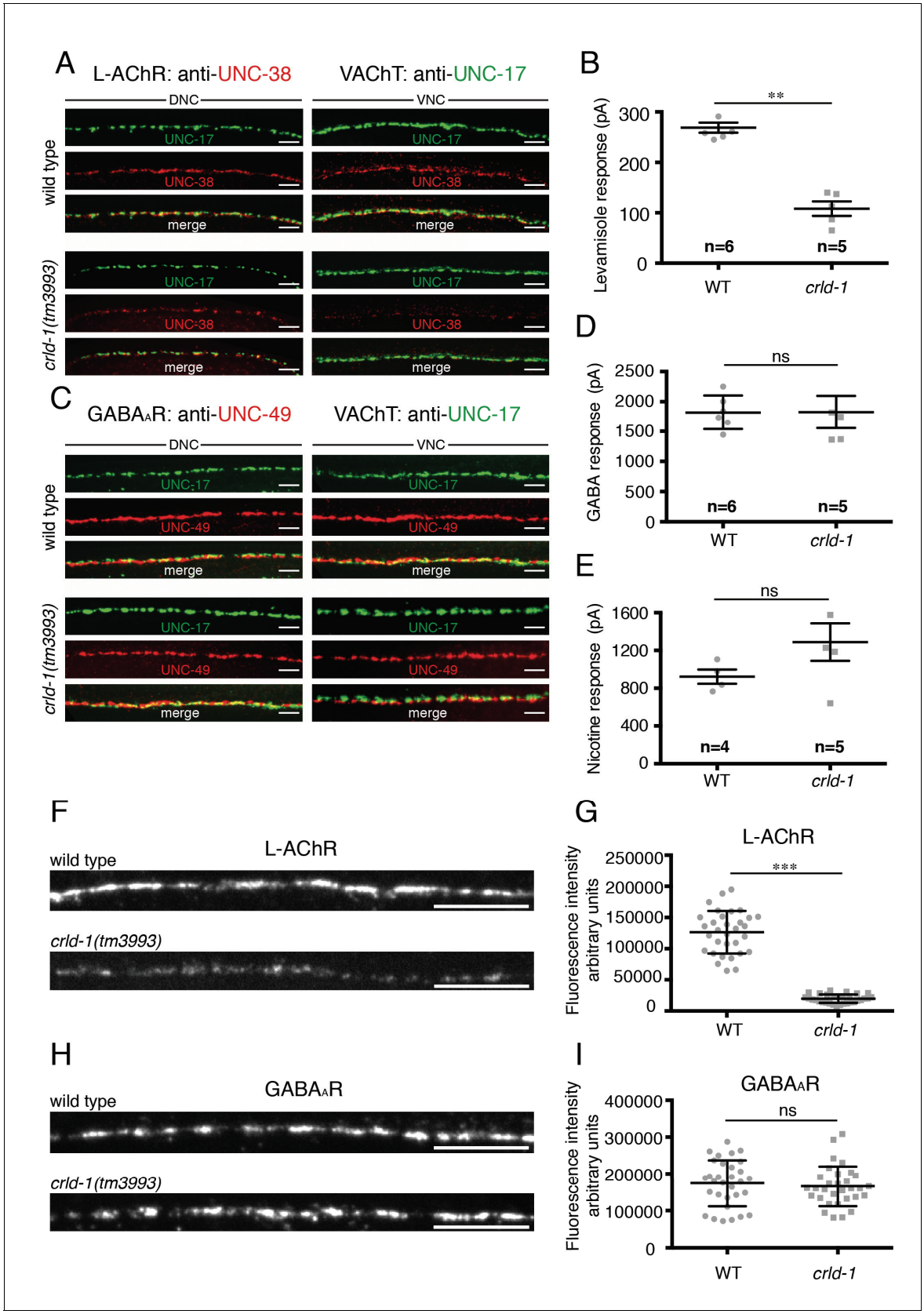

Figure 3. CRLD-1 is required for surface expression of L-AChRs. (**A**) L-AChR expression is decreased at NMJs of *crld-1(tm3993)* mutants, whereas presynaptic differentiation is unaffected. L-AChRs are labeled using anti-UNC-38. Cholinergic boutons are labeled using an anti-vesicular acetylcholine

Figure 3 continued on next page

Figure 3 continued

transporter UNC-17 (VAChT) antibody. DNC = dorsal nerve cord, VNC = ventral nerve cord. Scale bars 10 μm. (**B**) Response to pressure-ejection of levamisole in voltage-clamped ventral BWMs is reduced in *crld-1(tm3993)*. Data indicate mean ± SEM; WT: 269 ± 10 pA, n = 6 animals; *crld-1(tm3993)*: 108 ± 14 pA, n = 5 animals; p=0.0043. Mann-Whitney test. (**C**) $GABA_AR$ expression is unaffected at NMJs of *crld-1(tm3993)* mutants compared to wild type. $GABA_AR$ are labeled using anti-UNC-49 antibodies. Cholinergic boutons are labeled using anti-UNC-17 (VAChT) antibodies. DNC = dorsal nerve cord, VNC = ventral nerve cord. Scale bars 10 μm. (**D**) Electrophysiological response of body-wall muscle cells to pressure-ejection of GABA in *crld-1 (tm3993)* mutant is similar to the wild type. Data indicate mean ± SEM; WT: 1821 ± 115 pA, n = 6 animals; *crld-1(tm3993)*: 1826 ± 270 pA, n = 5 animals; p=0.6277, ns = not significant. Mann-Whitney test. (**E**) Response to pressure-ejection of nicotine in body wall muscles is unaffected in *crld-1(tm3993)*. Data indicate mean ± SEM; WT: 922 ± 76 pA, n = 4 animals; *crld-1(tm3993)*: 1289 ± 199 pA, n = 5 animals; p=0.1905, ns = not significant. Mann-Whitney test. (**F**) Confocal imaging of the L-AChR reporter UNC-29::tagRFP at the ventral nerve cords of wild-type and *crld-1(tm3993)* mutant adult worms. Scale bars = 10 μm. (**G**) Quantification of UNC-29::tagRFP fluorescence at the ventral nerve cords of wild-type and *crld-1(tm3993)* mutant adult worms. Data indicate mean ± SD; WT: n = 32 animals; *crld-1(tm3993)*: n = 32 animals; experiments were repeated three times.***p<0.001. Mann-Whitney test. (**H**) Confocal imaging of the $GABA_AR$ reporter UNC-49::tagRFP at the ventral nerve cords of wild-type and *crld-1(tm3993)* mutant adult worms. Scale bars = 10 μm. (**I**) Quantification of UNC-49::tagRFP fluorescence at the ventral nerve cords of wild-type and *crld-1(tm3993)* mutant adult worms. Data indicate mean ± SD; WT: n = 31 animals; *crld-1(tm3993)*: n = 31 animals; experiments were repeated three times. p=0.4068, ns = not significant. Mann-Whitney test.

DOI: https://doi.org/10.7554/eLife.39649.006

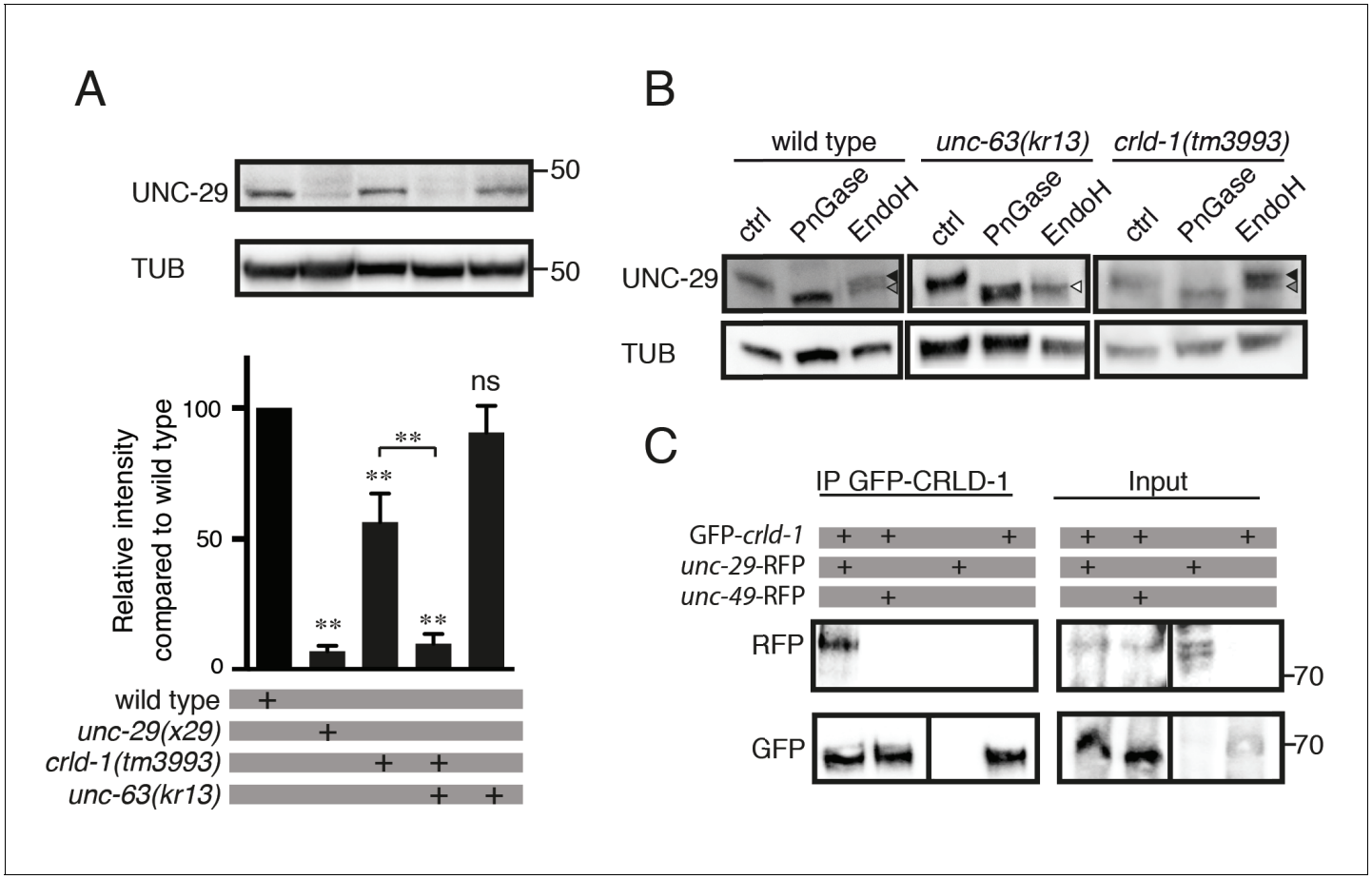

Figure 4. CRLD-1 is required for the stability of unassembled L-AChR subunits. (**A**) L-AChR expression is reduced in *crld-1(tm3993)* mutants. Levels of unassembled UNC-29 L-AChR subunits detected in *unc-63(kr13)* are further decreased in *unc-63(kr13);crld-1(tm3993)* double mutants. UNC-29 levels were quantified by western blot using anti-UNC-29 antibodies and normalized to tubulin levels. Significance is indicated compared to the wild type. The significance between *unc-63(kr13);crld-1(tm3993)* and *crld-1(tm3993)* is indicated by an horizontal line. Five independent experiments were quantified (mean ± SEM). p=0.6825, ns (not significant); **p=0.0079; after Bonferroni correction, Mann-Whitney test. TUB = tubulin. (**B**) Remaining L-AChRs exit the ER in *crld-1(tm3993)*. Treatments with EndoH or N-Glycosidase F (PNGase) were performed on protein extracts of mixed-stage animals before SDS-PAGE analysis. Black arrowheads indicate glycosylated forms resistant to EndoH, gray arrowheads indicate glycosylated forms partially resistant to EndoH, and white arrowheads indicate deglycosylated forms sensitive to EndoH. (**C**) CRLD-1 interacts with UNC-29 subunit of L-AChR in vivo. gfp-crld-1(kr298) animals were crossed with *rfp-unc-29(kr208)* or *rfp-unc-49(kr306)* to co-express CRLD-1 with RFP-tagged AChR or $GABA_AR$ subunits, respectively. Immunoprecipitation of GFP-CRLD-1 using GFP-Trap beads co-immunoprecipitated RFP-UNC-29, but not UNC-49-RFP. As a control, GFP-CRLD alone was not immunoprecipitated by anti-RFP antibody. A vertical line indicates that the lanes are not adjacent in the gel.
DOI: https://doi.org/10.7554/eLife.39649.007

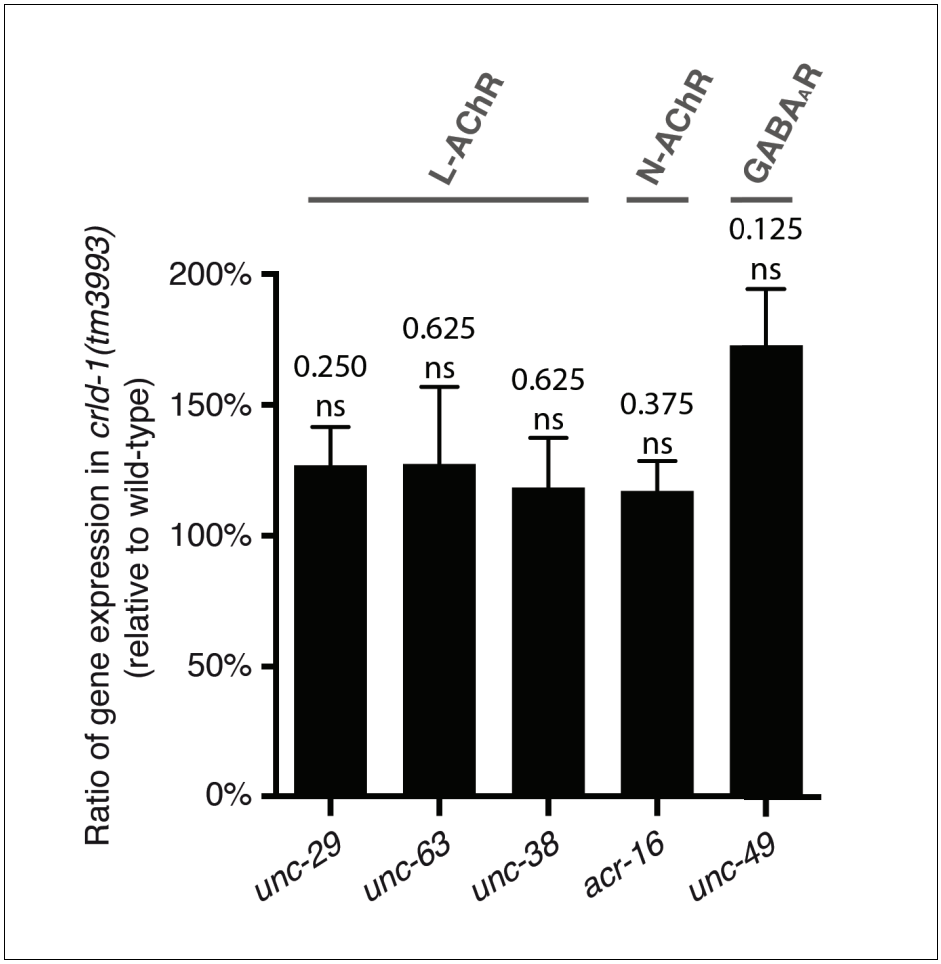

Figure 4—figure supplement 1. – Measurement of L-AChR subunit mRNA levels. Transcript levels of ionotropic receptor subunits are not significantly decreased in *crld-1(tm3993)*. Quantitative real-time PCR measurements of mRNA levels for heteromeric levamisole-sensitive AChRs (L-AChR; *unc-29*, *unc-63*, and *unc-38*), homomeric nicotine-sensitive AChRs (N-AChR; *acr-16*), and $GABA_A$ receptors (*unc-49*). mRNA samples were collected from synchronized L4 larvae. Fold-change, mean ± SEM in *crld-1(tm3993)* relative to WT is shown in four independent experiments. P values are indicated on the figure, ns (not significant), after Bonferroni Holm correction, Wilcoxon signed-rank test.

DOI: https://doi.org/10.7554/eLife.39649.008

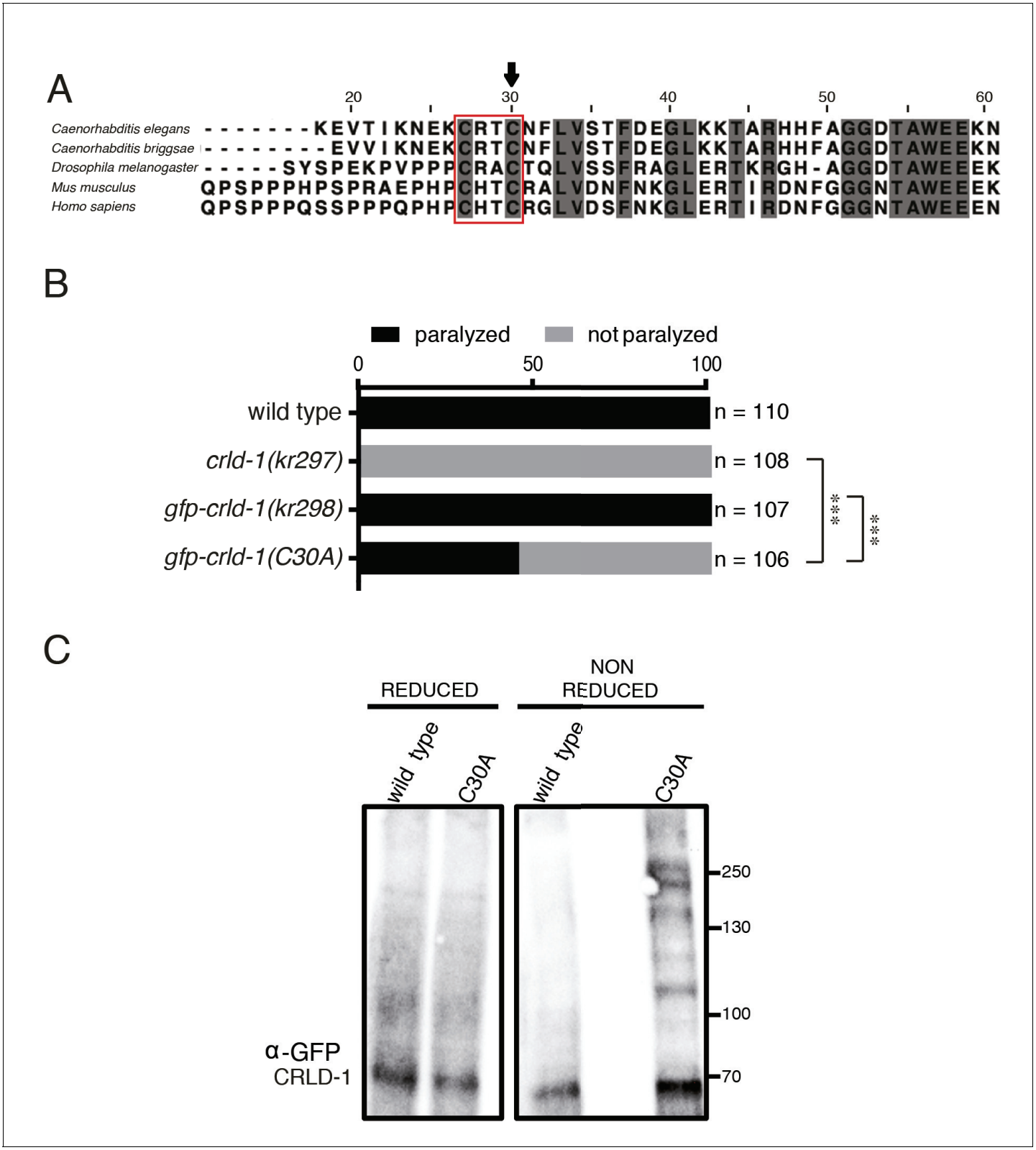

Figure 5. CRLD-1 displays putative PDI-like activity. (**A**) ClustalO alignment of *C. elegans* CRLD-1 with orthologous CRLD proteins from nematodes, fly, and vertebrates. The conserved CXXC motif present in the WE domain is boxed. Identical residues conserved in all species are highlighted in dark gray. The position of the cysteine residue that was mutated to generate the C30A mutation in *gfp-crld-1(C30A)* knock-in worms is indicated by an arrow. (**B**) Animals expressing the C30A mutation in the *crld-1* gene display partial levamisole resistance. Gray bars indicate the percentage of moving

Figure 5 continued on next page

Figure 5 continued

animals after overnight exposure to 1 mM levamisole, and black bars indicate the percentage of paralyzed animals. Experiments were repeated three times, n = number of animals tested. ***p<0.001, after Bonferroni correction, Fisher exact probability test. (**C**) The substrate-trapping CRLD-1 C30A mutant formed high molecular weight mixed disulphide complexes that were resolved under reducing conditions. In contrast, wild-type CRLD-1 did not form higher molecular weight complexes with putative substrate proteins. Total protein extract from *gfp-crld-1(kr298)* wild-type and *gfp-crld-1(kr302)* C30A mutant worms were separated by SDS-PAGE followed by Western blot analysis for GFP to detect CRLD-1.

DOI: https://doi.org/10.7554/eLife.39649.009

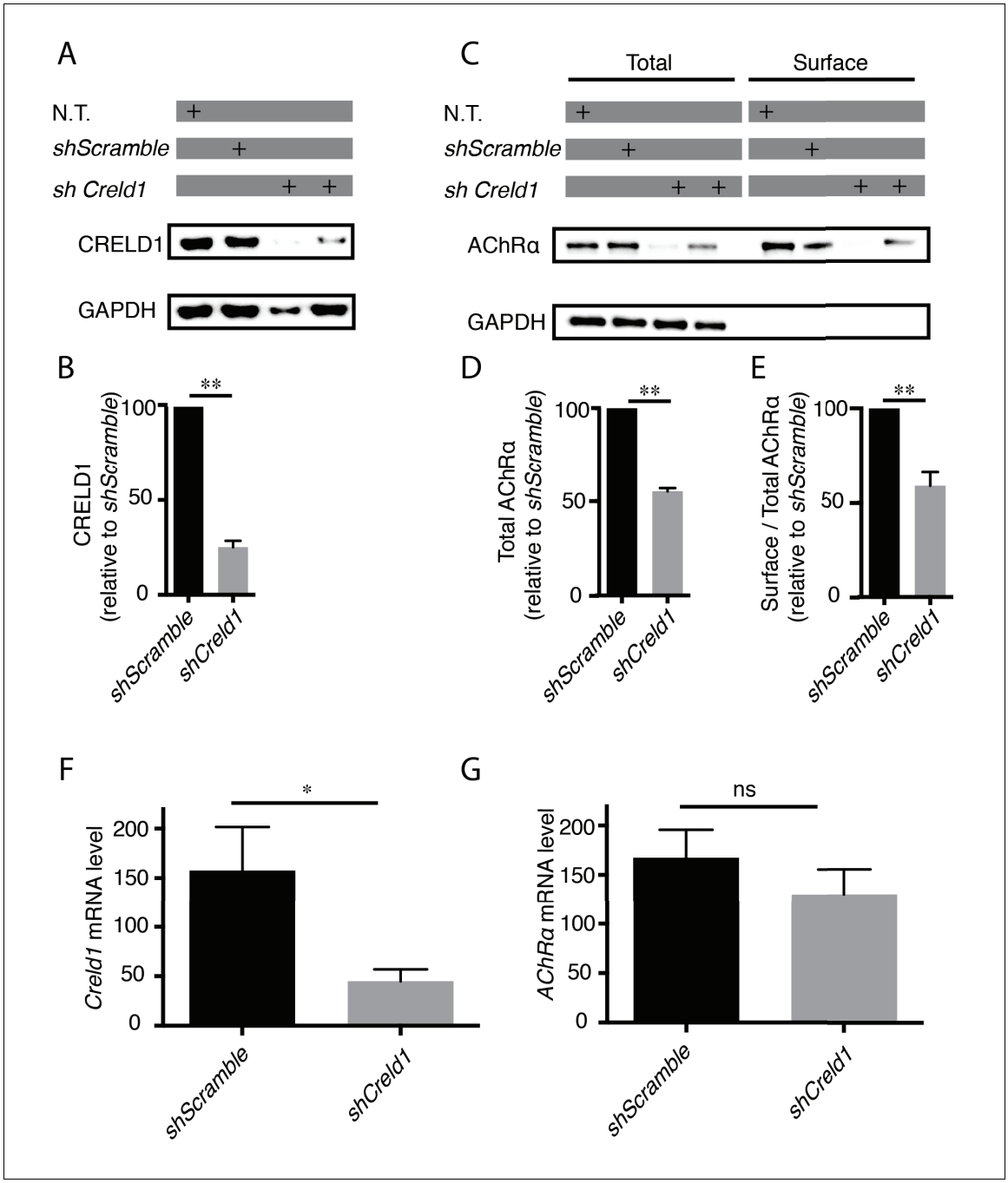

Figure 6. *Creld1* knockdown leads to reduced AChR expression at the plasma membrane *in vitro*. (**A–E**) Measurement of mouse CRELD1 and AChR α subunit protein levels. C2C12 cells expressing shRNA against *Creld1* (*shCreld1*) or scrambled (*shScramble*) sequences were differentiated for 5 days and then subjected to surface labeling with αBT-biotin for AChRα. N.T. = non transfected cells. Streptavidin precipitates (surface) and total lysates were separated by SDS/PAGE and probed for indicated proteins (**A and C**). CRELD1 protein levels were reduced by 75% in cells expressing *shCreld1* as compared to *shScramble* (**B**). Quantitation of total AChRα levels (**D**) and of the surface to total AChRα ratio (**E**) in *shScramble* (100%) and *shCreld1* cells from n = 5 independent experiments. Error bars, SEM; **p=0,0079, Mann-Whitney test. (**F–G**) Measurement of mouse *Creld1* and *AChRα* subunit mRNA levels. C2C12 cells expressing *shScramble* or *shCreld1* were differentiated for 5 days and then subjected to RNA extraction. Quantitative real-time PCR measurements of mRNA levels for *Creld1* (**F**) and *AChRα* subunit (**G**). *Creld1* mRNA is decreased in *shCreld1* cells compared to *shScramble* cells, whereas *AChRα* subunit

Figure 6 continued on next page

Figure 6 continued

mRNA is not significantly decreased in *shCreld-1* cells. Mean ± SEM is shown in six independent experiments. *p=0,0411; p=0,4740, ns (not significant), Mann–Whitney test.

DOI: https://doi.org/10.7554/eLife.39649.010

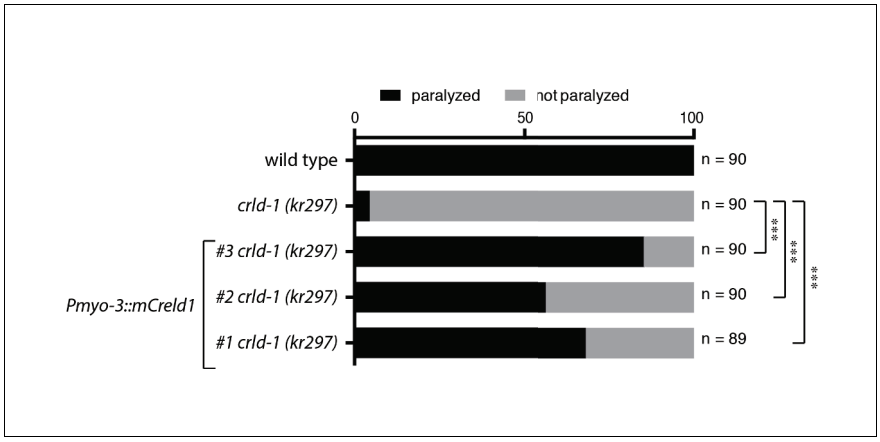

Figure 6—figure supplement 1. Mouse *Creld1* rescues levamisole-sensitivity of *crld-1* mutant worms. Expression of mouse *Creld1* in *C. elegans* muscle cells under the control of the *Pmyo-3* promoter rescues levamisole sensitivity in *kr297* mutants. Gray bars indicate the percentage of moving animals after overnight exposure to 1 mM levamisole, and black bars indicate the percentage of paralyzed animals. three independent transgenic lines were tested. Experiment was repeated three times, n = number of animals tested. ***p<0.001, after Bonferroni correction, Fisher exact probability test.

DOI: https://doi.org/10.7554/eLife.39649.011

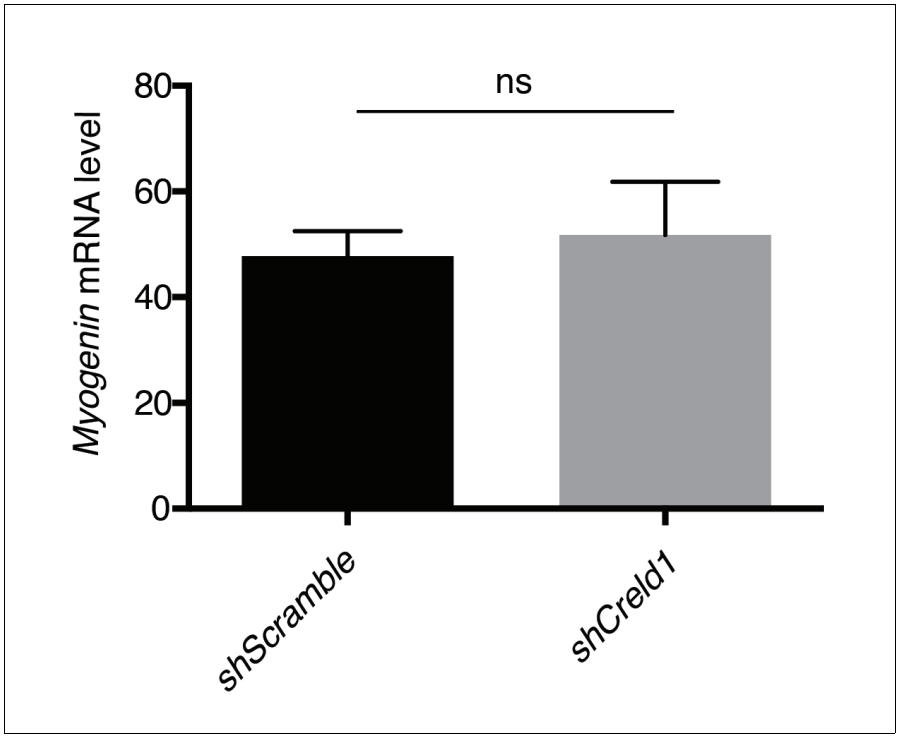

Figure 6—figure supplement 2. Knocking down *Creld1* does not impact *Myogenin* transcriptional levels. C2C12 cells expressing *Scramble* or *Creld1* shRNA were differentiated for 5 days, and then subjected to RNA extraction. Quantitative real-time PCR measurements of mRNA levels shows that *Myogenin* is not significantly decreased in *shCreld-1* cells. Fold-change, mean ± SEM in *shCreld-1* relative to *shScramble* (100%) is shown in four independent experiments. p>0,9999, ns (not significant), Mann–Whitney test.

DOI: https://doi.org/10.7554/eLife.39649.012